Local-mode dynamics in YH_2 and YD_2 by isotope-dilution neutron spectroscopy

T. J. Udovic and J. J. Rush
Materials Science and Engineering Laboratory, National Institute of Standards and Technology, Gaithersburg, Maryland 20899

I. S. Anderson
Institut Laue-Langevin, 38042 Grenoble Cedex, France

(Received 12 July 1994; revised manuscript received 16 August 1994)

Isotope-dilution neutron spectroscopy was used to investigate the dynamics of the H and D optic vibrations in YH_2 and YD_2, respectively. The broad, complex, densities of states of the tetrahedrally coordinated H and D atoms in the isotopically pure materials collapse to single, sharp, triply degenerate features when the H and D atoms are sufficiently diluted with their companion isotopes. This demonstrates that the vibrational dispersion for the pure materials is due to the presence of significant H-H and D-D dynamic-coupling interactions. Moreover, a spectral doublet (with 5-meV splitting) superimposed on the sharp D-defect-mode feature for $Y(H_{0.9}D_{0.1})_2$ is suggestive of localized acoustic and optic branches of dynamically coupled, near-neighbor D-D pairs isolated in the predominantly hydrided material. The magnitude of the splitting implies a D-D/Y-D force-constant ratio of $\sim 6\%$. The dynamics of both light (H) and heavy (D) mass defects are in general agreement with simple mass-defect theory.

INTRODUCTION

Yttrium dihydride (β-YH_2) is among a group of rare-earth and other metal dihydrides possessing a CaF_2 structure[1] where the hydrogen atoms fully populate the interstitial tetrahedral (t site) sublattice created by the face-centered-cubic lattice of metal atoms. In this structure, each t-site hydrogen is situated in an identical local cubic environment, which in the absence of H-H interactions would lead to a sharp, triply degenerate, optic-mode vibrational spectrum. In reality, the vibrational density of states (DOS) as measured by incoherent inelastic neutron scattering (IINS) (e.g., Refs. 2–4) was found to possess a much broader than expected line shape of considerable complexity. This line shape was originally shown by simple central-force, lattice-dynamics calculations[5] to stem from the presence of significant hydrogen-hydrogen interactions within the tetrahedral sublattice. Subsequent coherent inelastic neutron-scattering measurements[6,7] of the optic-phonon dispersion relations for single-crystal β-$CeD_{2.12}$ led to more-involved calculations utilizing bond-bending force constants and longer-range interactions in an attempt to model the results. Very few metal hydrides, however, can be produced in single-crystal form, which complicates the study of detailed force fields and dynamic interactions.

In recent years, the use of IINS with hydrogen and deuterium comixtures in condensed-phase materials has been found to be a potent combination for investigating the presence and degree of H-H interactions. In particular, isotope-dilution neutron spectroscopy (IDNS) has been used successfully as a probe of the dynamic H-H interactions for such systems as β-PdH_x (Ref. 8) and α-YH_x,[9] as well as for adsorbed hydrogen on Pt black,[10] Pd black,[11] and RuS_2.[12] In IDNS experiments, materials are synthesized using a mixture of H and D isotopes while maintaining the same (H+D)/metal ratio. By using a large D/H ratio, hydrogen is isotopically diluted with deuterium to form isolated H atoms within the material. The difference in mass between H and D effectively inhibits its dynamic coupling which would otherwise occur between each isolated H atom and its vicinal D atoms if significant H-D interactions were present. Hence, for a particular hydrogen normal mode, a broad, complex vibrational band that is predominantly due to H-H interactions in the pure hydride will be reduced to a much sharper feature in the corresponding isotopically diluted material from the dynamically isolated H defects residing in their locally identical environments. Since each H defect possesses three orthogonal normal-mode vibrations, there are potentially three nondegenerate vibrational energies for each type of hydrogen interstitial site. The identical cubic symmetry surrounding each t-site hydrogen in YH_2 means that the corresponding H-defect spectrum would, in principle, display a single, triply degenerate feature. Conversely, the presence of additional features would indicate that the symmetry is less than cubic and/or there is more than one type of hydrogen interstitial site populated. Thus, by employing IDNS to "tune out" the complicating dynamic-coupling effects of H-H interactions present in many materials such as metal hydrides, one can also obtain useful structural information concerning H-site geometry. In this paper, isotope-dilution neutron spectroscopy is used to investigate the origin of the complex DOS for the optic vibrations of the t-site H and D atoms in YH_2 and YD_2.

EXPERIMENTAL PROCEDURE

Preparation of $Y(H_xD_{1-x})_2$ samples followed a procedure[13] similar to that established by Vajda, Daou, and Burger.[14] Starting with 4–18 g lots of high-purity Y

(99.99 at. %, Johnson Matthey), samples were loaded with H_2 (Matheson Research grade) and D_2 (Spectra Gases Research Grade) by gas-phase absorption in a quartz tube. The fully deuterated sample was synthesized using higher isotopic purity D_2 (Cambridge Isotope Laboratories, 99.98% D). Except for $x=0.9$, the "ideal" $Y(H_xD_{1-x})_2$ compounds were prepared by loading with premixed gases to a nominal (H+D)/Y ratio of 2.005 at 873 K to ensure full t-site occupation, followed by evacuation at 773 K to remove any excess octahedrally coordinated (o site) hydrogen, which is unstable at this temperature.[14] The $Y(H_{0.9}D_{0.1})_2$ sample was prepared by first hydrogen loading to a H/Y ratio of 1.80 at 1073 K followed by deuterium loading to a D/Y ratio of 0.20, cooling to 1023 K and allowing to equilibrate for 16 h, and finally evacuating at 773 K. After cooling to room temperature, all the samples were transferred to a He-filled glove box, pulverized, and loaded into thin Al-plate cells. All measurements were performed below 10 K using the BT-4 spectrometer at the Neutron Beam Split-Core Reactor at the NIST. Two instrumental configurations with the Cu(220) monochromator were used. The low-resolution configuration consisted of 40'-40' collimations and a Be-filter analyzer, yielding a full width at half maximum (FWHM) resolution δE that increased from ~6 to 7% of the energy loss E as E increased from 80 to 200 meV. The high-resolution configuration consisted of 20'-20' collimations and a composite Be-graphite-Be-filter analyzer, yielding a $\delta E/E$ that increased from ~2.4 to 2.8% as E increased from 80 to 140 meV. The resolution is depicted in the figures by horizontal bars. All illustrated spectra are corrected for the fast-neutron background. The spectra are not normalized with respect to concentration or integrated intensity; rather, relative scales are adjusted solely for the purpose of clarity.

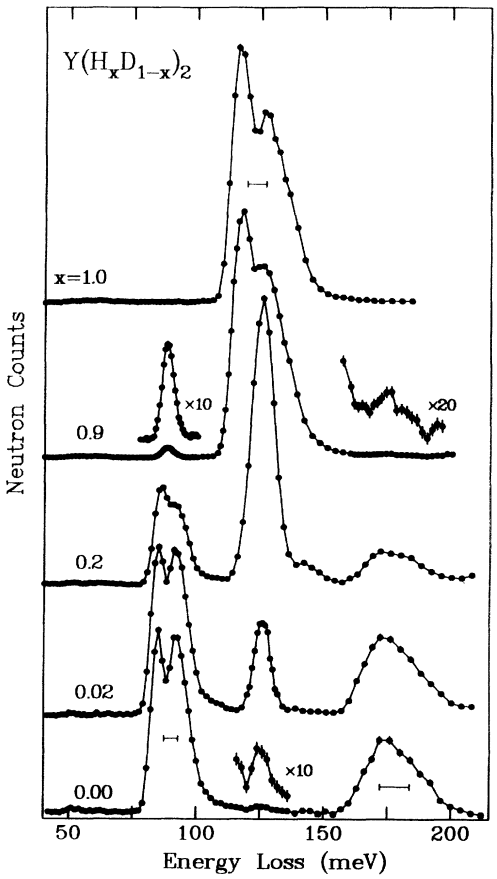

FIG. 1. Low-resolution vibrational spectra of $Y(H_xD_{1-x})_2$ for various values of x. Lines through the spectra are drawn as guides to the eye.

RESULTS AND DISCUSSION

Figure 1 shows the low-resolution optic-vibrational spectra of YH_2, YD_2, and a range of isotopically diluted samples. The DOS of the t-site hydrogen and deuterium in the isotopically pure samples possess significant fine structure and are clearly much broader than the instrumental resolution. These spectra are typical of the CaF_2-type dihydrides, and in particular, the t-site spectrum for YH_2 is in agreement with that reported previously.[4] The H and D optic bands display a bimodal structure centered at ~123 and 90 meV, respectively. The multiphonon "overtone" corresponding to the D optic band is evident at ~175 meV. Dilution of the isotopically pure samples produces dramatic transformations of the DOS. In both cases, the optic-band broadening disappears and is replaced by a sharp defect-mode feature. These transformations appear even more pronounced when measured under high-resolution conditions, as illustrated in Fig. 2. The H- and D-defect mode energies are found by Gaussian fits to be 126.2 and 88.1 meV, respectively. The observed D-defect overtone at ~175 meV for $x=0.9$ in Fig. 1 indicates the approximate harmonic nature of the t-site potential. This behavior of the t-site DOS with isotope dilution clearly demonstrates that the

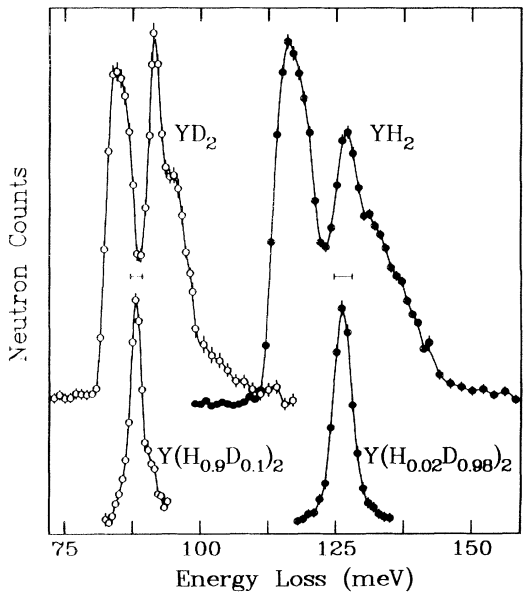

FIG. 2. High-resolution vibrational spectra of $Y(H_xD_{1-x})_2$ for various values of x. Lines through the spectra are drawn as guides to the eye.

broadening in the isotopically pure samples is entirely a manifestation of H-H and D-D dynamic interactions as opposed to the presence of H and D absorbed in more than one type of interstitial site and/or in a t site with less than cubic local symmetry.

It is interesting to note the effects of varied dilution on the DOS of $Y(H_xD_{1-x})_2$. For example, for $x=0.2$, each H atom is not sufficiently diluted with D to be completely isolated from the other H atoms. In this case, minor contributions from H-H interactions tend to smear out the H-defect feature, as seen in Fig. 1. Increasing the degree of dilution further to $x=0.02$ more completely isolates the H defects leading to a sharper feature than for $x=0.2$. The narrowness of this feature is emphasized by the high-resolution spectrum in Fig. 2. It is also striking to note the sharp H-defect feature evident even in the sample with $x=0.00$ (Fig. 1). Even though the actual isotopic purity of the gas used was 99.98% D, the intensity of the H-defect feature indicates that, in reality, the H fraction is larger than expected with $x\approx 0.001$. This is not unreasonable, since some residual H in the original metal sample and/or from the gas-absorption apparatus can easily explain the minute yet larger than expected fraction of H in the deuterated sample.

The effects of finite dilution are also evident for the D-defect feature for $x=0.9$ in Fig. 2, where the high resolution allows one to discern both higher- and lower-energy wings roughly coinciding with the major features in the YD_2 spectrum. These wings likely represent the bimodal DOS due to the local "acoustic" and "optic" modes along the bond axis of nearest-neighbor D-D defect pairs, similar to that previously observed[9,15] for D-D and H-H c-axis-directed pairs present in α-YD_x and α-YH_x solid solutions. Figure 3 shows a multicomponent Gaussian fit of the D-defect spectrum. All features were constrained to have identical widths and the components of the doublet were constrained to have the same intensity. This yielded a fitted width of 2.2-meV FWHM, which was very close to the instrumental resolution. The positions of the acoustic and optic modes were located at 85.7 and 90.8 meV, respectively, split by ~ 5 meV. A comparison of the peak intensities yielded a $D_{\text{paired}}/D_{\text{isolated}}$ vibrational intensity ratio of 0.39.

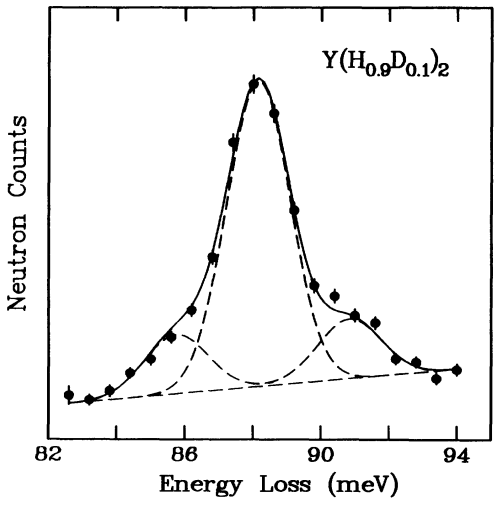

FIG. 3. Multicomponent Gaussian fit (solid curve) of the high-resolution, D-defect-mode, vibrational spectrum for $Y(H_{0.9}D_{0.1})_2$. Component features are indicated by the dashed curves. The central peak represents isolated D atom vibrations; the doublet represents the acoustic and optic components of D-D pair vibrations. Details are described in the text.

One can calculate the theoretical intensity ratio upon the assumption that the D vibrations along the three principal (and orthogonal) crystallographic directions are independent of each other and statistically identical. Hence the statistical problem becomes one-dimensional and one need only consider the arrangement of D and H atoms along any one crystallographic axis. In this case, one can equate the $D_{\text{paired}}/D_{\text{isolated}}$ intensity ratio to the probability that a given D atom is a member of a D-D pair, divided by the probability that it is isolated. The probability that a D atom is isolated is just x^2, which is the probability that both nearest-neighbor t sites are occupied by H atoms. The probability that a D atom is a member of a D-D pair (and not a D-D-D triplet, etc.) is equal to $2x^2(1-x)$, which is the probability that only one of the nearest-neighbor t sites is occupied by a D atom, which in turn is followed by an H atom. Thus, the theoretical $D_{\text{paired}}/D_{\text{isolated}}$ intensity ratio $=2(1-x)=0.2$, roughly half of what is observed. If one considers all other nonisolated D atoms (e.g., D-D-D triplets, etc.) as also contributing to the paired D DOS, then the theoretical ratio becomes the probability that a D atom is nonisolated, divided by the probability that it is isolated. Noting that the sum of the probabilities of an isolated and nonisolated D atom is unity, the $D_{\text{nonisolated}}/D_{\text{isolated}}$ intensity ratio $=(1-x^2)/x^2=0.23$, which is close to the case considering only D-D pairs and still much smaller than observed.

Due to the different synthesis procedure used for this sample (i.e., sequential addition of H_2 and D_2 followed by high-temperature equilibration), it is certainly possible that the split DOS feature due to paired D atoms is enhanced by incomplete statistical mixing of the D and H isotopes among the t sites. The observed $D_{\text{paired}}/D_{\text{isolated}}$ intensity ratio of 0.39, when equated to $2(1-x)$, yields an effective D fraction of $(1-x)=0.2$, which is twice the actual value. The hydrogen diffusion coefficients reported[16,17] for β-YH_2 indicate that the H and D mobilities are relatively slow even at 1023 K, suggesting that isotopic mixing, especially within the larger metal-hydride grains in our sample, may not be complete. Alternatively, although less likely, it is conceivable that the D-defect atoms in the predominantly YH_2 lattice are indeed statistically mixed, yet have a tendency toward forming D-D pairs. In the limit of a complete pairing of all D defects, one of the three orthogonal vibrations for each D atom would be a pairlike vibration along the D-D axis; the other two would be degenerate vibrations perpendicular to the D-D axis and akin to those of an isolated D defect, since in these directions, the D atom has only H nearest neighbors. In this situation, one would obtain a $D_{\text{paired}}/D_{\text{isolated}}$ intensity ratio of 0.5, which is larger than but closer to what is observed. Further measurements of

the same sample, after attempting a more prolonged isotopic mixing at high temperature, as well as additional new samples with appropriate isotope ratios carefully synthesized with premixed gases are needed to clarify the cause of the larger than expected $D_{\text{paired}}/D_{\text{isolated}}$ intensity ratio.

Leaving aside the nonideal intensity ratios, one can apply a simple, one-dimensional, coupled-harmonic-oscillator model, similar to that used previously to describe the spectroscopic splitting along the c direction for α-YH_x,[9] to define a splitting $\Delta E \approx E_a \kappa/k$, where E_a is the energy of the acoustic mode (i.e., the lower-energy component), κ is the D-D coupling force constant, and k is the Y-D force constant. This model also predicts that the energy of the isolated D vibrations bisects the pairing-induced doublet at $E_{\text{isolated}} = E_a + \Delta E/2$, which is consistent with what is observed. Upon substitution of the measured splitting and acoustic-mode energy into the model, one obtains $\kappa/k \approx \Delta E/E_a = 0.06$, implying that the D-D coupling constant is $\sim 6\%$ of the Y-D force constant. This is consistent with the value of $6.6 \pm 0.9\%$ determined from the analysis of the optic-phonon dispersion curves of single-crystal $CeD_{2.12}$.[6] It should be further noted that the D-D coupling constant determined for next-nearest-neighbor D atoms in the $CeD_{2.12}$ study[6] was a factor of 10 lower than that found for nearest-neighbor D atoms. Assuming a similar ratio in the present case, this translates into an expected spectroscopic splitting for next-nearest-neighbor D-D pairs of ~ 0.5 meV, which is too small to be resolved with the current instrumental resolution. Hence, this further justifies our assertion that the observed 5-meV spectral splitting is due to the interaction of nearest-neighbor D-D pairs.

Efforts to extract similar quantitative information about H-H pair vibrations from the H-defect DOS for $x = 0.02$ in Fig. 2 were limited by the lower proportion of H-H pairs, the poorer instrumental resolution (3.4-meV FWHM) at 126-meV energy transfer, and the narrow energy range scanned. A slight broadening of the H-defect peak is evident, but a quantitative study of H-H pairs will require measuring isotopically dilute systems with slightly larger x values (to increase the relative proportion of H-H pairs) over a larger energy range and with somewhat better instrumental resolution.

Besides the effects on the defect features, the degree of isotope dilution also influences the host DOS. For $x = 0.2$, the D-host DOS in Fig. 1 exhibits a less-prominent fine structure compared to that for YD_2, due to a breakup of the perfect D-host sublattice by the significant fraction of H defects. This is also evident for the H-host DOS with $x = 0.9$, and to a lesser extent, even for the D-host DOS with $x = 0.02$.

We have also applied simple mass-defect theory to describe the IDNS results. According to this theory, the dynamics of the isolated H or D defect (d) atoms diluted within the otherwise pure host (h) sublattice of the companion D or H isotopes are described by[18,19]

$$\int \frac{g_h(E)dE}{E_d^2 - E^2} = \frac{1}{\epsilon E_d^2} , \tag{1}$$

where $g_h(E)$ is the energy-dependent DOS of the host phase normalized so that $\int g_h(E)dE = 1$, E_d is the local-mode energy of the defect, and $\epsilon = (m_h - m_d)/m_h$, where m_h and m_d are the masses of the host and defect atoms, respectively. In effect, this equation indicates that the defect atom tends not to vibrate within the dispersion-broadened DOS of the surrounding host atoms [i.e., $E_d^2 - E^2$ in Eq. (1) would become zero at $E = E_d$, making the integral too large to equate to the right-hand side]. Rather, the defect undergoes a localized vibration that is detached from the host phonon band and involves the participation of only a few neighboring atoms. For the case of lighter H-defect atoms surrounded by heavier D-host atoms, $\epsilon = \frac{1}{2}$, and the H-defect mode must be located *above* the energy cutoff for $g_D(E)$. Conversely, for the case of heavier D-defect atoms surrounded by lighter H-host atoms, $\epsilon = -1$, and a D-defect mode must be located *below* the energy cutoff for $g_H(E)$. This effect is visually evident from a comparison of the positions of the H- and D-defect modes relative to the broad H and D vibrational bands of YH_2 and YD_2 in Fig. 2. The H- and D-defect-mode energies of 130.2 and 87.1 meV were calculated from Eq. (1) by an iterative process using the appropriately normalized high-resolution spectra of YH_2 and YD_2 in Fig. 2 as the host DOS. An attempt was made to improve this calculation by excluding the estimated contribution of the multiphonon high-energy tails from the DOS used in the calculation. The resulting defect-mode energies of 127.8 and 86.6 meV were still only in fair agreement with the corresponding experimental values of 126.2 and 88.1 meV, and in effect, overestimate the upward shift of the H-defect mode and the downward shift of the D-defect mode away from their respective host DOS. Lack of exact agreement is not unexpected since simple mass-defect theory is based on the ideal assumptions that the t-site potential is harmonic and the lattice constants and interatomic force constants are identical for YH_2 and YD_2. The ratio of the overtone energy to the main D-defect mode energy for $x = 0.9$ in Fig. 1 of 1.99 implies that the t-site potential is indeed very close to harmonic. Yet, the DOS for YH_2 and YD_2 overlap by multiplying the YD_2 energy scale by a factor of ~ 1.38, smaller than the ideal factor of 1.41. This is consistent with the fact that the lattice constant for YD_2 (0.5195 nm, at room temperature)[20] is $\sim 0.25\%$ smaller than that for YH_2 (0.5208 nm),[20,21] which should result in slightly stiffer interatomic force constants for YD_2. The ideal result for identical interatomic force constants is easily seen from Eq. (1) for the situation where the host DOS $g_h(E)$ is a δ function at E_h (i.e., no H-H or D-D interactions). In this case, the equation simplifies to $E_h^2/E_d^2 = 1 - \epsilon = m_d/m_h$, which yields $E_H/E_D = \sqrt{2}$ as expected for either isotope-dilution case. Hence, the small deviations of the data from simple mass-defect theory suggest that, although nearly harmonic, the t-site potentials of the defect atoms differ slightly from those of the host atoms. The presence of the defect atoms causes a perturbation of the corresponding t site. For D defect atoms, the corresponding t site contracts slightly compared to the rest of the lattice, causing a local stiffening of the in-

teractions of the D defect with its Y and H neighbors. On the contrary, for H-defect atoms, the corresponding t site expands slightly compared to the rest of the lattice, causing a local softening of the interactions of the H defect with its Y and D neighbors.

It is interesting to incorporate these nonidealities into an "effective" ϵ, $\epsilon_{\text{eff}}=1-(m_d/m_h)_{\text{eff}}\approx 1-(m_d/k_d)/(m_h/k_h)$, where $(m_d/m_h)_{\text{eff}}$ is an effective-mass ratio of the defect and host isotopes that compensates in a somewhat crude fashion for the differences in the force constants, k_d and k_h, involving the defect and host atoms, respectively. The effective mass ratio is extracted from the value of ϵ_{eff} determined from Eq. (1) using the experimentally observed D- and H-defect energies. This provides a rough measure of the force-constant perturbations induced by the defects compared to the isotope-dependent differences in force constants observed in the isotopically pure materials. This approach yields an $(m_{\text{D}}/m_{\text{H}})_{\text{eff}}$ ratio of ~ 1.94 for both types of defects. Although smaller than 2, it is somewhat larger than the value of $(1.38)^2=1.90$ calculated from the square of the energy-scale factor that was necessary for spectral overlap of the YD_2 and YH_2 DOS. From these results, we estimate $k_{\text{H}}/k_{\text{D}}$ values ≈ 0.97 for both types of isotopically dilute samples and ≈ 0.95 (assuming a harmonic model where $E_{\text{H}}^2/E_{\text{D}}^2=[(k_{\text{H}}/m_{\text{H}})/(k_{\text{D}}/m_{\text{D}})]$ for the isotopically pure materials. This suggests that the force constants associated with the defect atoms are indeed perturbed with respect to those of the host lattice but the differences are not as pronounced as the difference in interatomic force constants associated with H and D in the isotopically pure materials. Thus in the isotopically dilute samples, the host lattice appears to mitigate yet not completely prevent changes in the size of the t sites containing the defect atoms.

SUMMARY

The power of IDNS to probe H-H interactions in condensed-phase materials has been exemplified. The data can be characterized reasonably well by simple mass-defect theory and clearly demonstrate that significant interactions in the t-site sublattice of YH_2 and YD_2 are the cause of the observed optic-band broadening. The 5-meV spectral splitting associated with isolated D-D pairs implies a D-D/Y-D force-constant ratio of $\sim 6\%$. On a more general note, this study illustrates the capability of IDNS to investigate the behavior of heavy D mass defects in an otherwise purely hydrided material, which to our knowledge has not previously been attempted because of the much larger neutron-scattering cross section for H compared to D. This capability should have many applications in future studies of metal hydride and hydrogenous molecular systems.

[1] D. Khatamian, W. A. Kamitakahara, R. G. Barnes, and D. T. Peterson, Phys. Rev. B **21**, 2622 (1980).

[2] S. S. Pan, W. E. Moore, and M. L. Yeater, Trans. Am. Nucl. Soc. **9**, 495 (1966).

[3] J. J. Rush, H. E. Flotow, D. W. Connor, and C. L. Thaper, J. Chem. Phys. **45**, 3817 (1966).

[4] J. A. Goldstone, J. Eckert, P. M. Richards, and E. L. Venturini, Solid State Commun. **49**, 475 (1984).

[5] E. L. Slaggie, J. Phys. Chem. Solids **29**, 923 (1968).

[6] C. J. Glinka, J. M. Rowe, J. J. Rush, G. G. Libowitz, and A. Maeland, Solid State Commun. **22**, 541 (1977).

[7] P. Vorderwisch, S. Hautecler, and W. D. Teuchert, Solid State Commun. **25**, 213 (1978).

[8] J. J. Rush, J. M. Rowe, and D. Richter, Phys. Rev. B **31**, 6102 (1985).

[9] I. S. Anderson, N. F. Berk, J. J. Rush, and T. J. Udovic, Phys. Rev. B **37**, 4358 (1988).

[10] J. J. Rush, R. R. Cavanagh, R. D. Kelley, and J. M. Rowe, J. Chem. Phys. **83**, 5339 (1985).

[11] J. M. Nicol, T. J. Udovic, J. J. Rush, and R. D. Kelley, Langmuir **4**, 294 (1988).

[12] W. H. Heise, K. Lu, Y.-J. Kuo, T. J. Udovic, J. J. Rush, and B. J. Tatarchuk, J. Phys. Chem. **92**, 5184 (1988).

[13] T. J. Udovic, J. J. Rush, and I. S. Anderson, Phys. Rev. B **50**, 7144 (1994).

[14] P. Vajda, J. N. Daou, and J. P. Burger, Phys. Rev. B **36**, 8669 (1987).

[15] I. S. Anderson, J. J. Rush, T. Udovic, and J. M. Rowe, Phys. Rev. Lett. **57**, 2822 (1986).

[16] U. Stuhr, M. Schlereth, D. Steinbinder, H. Wipf, B. Frick, and A. Magerl, Z. Phys. Chem. Neue Folge **164**, 929 (1989).

[17] K. J. Barnfather, E. F. W. Seymour, G. A. Styles, A. J. Dianoux, R. G. Barnes, and D. R. Torgeson, Z. Phys. Chem. Neue Folge **164**, 935 (1989).

[18] S. W. Lovesey, in *Frontiers of Physics,* edited by D. Pines (Benjamin Cummings, Reading, MA, 1980), Vol. 49.

[19] R. J. Elliot and A. A. Maradudin, in *Inelastic Scattering of Neutrons* (IAEA, Vienna, 1965), Vol. 1, p. 231.

[20] J. H. Weaver, R. Rosei, and D. T. Peterson, Phys. Rev. B **19**, 4855 (1979).

[21] M. Chiheb, J. N. Daou, and P. Vajda, Z. Phys. Chem. **179**, 255 (1993).